This article is published as: T. Bartelds, A. Capra, S. Hamaza, S. Stramigioli and M. Fumagalli, "Compliant Aerial Manipulators: Toward a New Generation of Aerial Robotic Workers," in IEEE Robotics and Automation Letters, vol. 1, no. 1, pp. 477-483, Jan. 2016. doi: 10.1109/LRA.2016.2519948 © 2016 IEEE

Compliant Aerial Manipulators: Towards a New Generation of Aerial Robotic Workers

J.T. Bartelds, A. Capra, S. Hamaza, S. Stramigioli and M. Fumagalli

***Abstract*— This paper focuses on the problem of handling impacts by means of an aerial manipulator and proposes a solution that combines the control of the aerial manipulator's end-effector position with an innovative manipulation system consisting of both active and passive joints. The approach aims at limiting the influence of impacts on the controlled attitude dynamics in order to allow the aerial manipulator to remain stable during and after impact. The developed concept is intended to convert kinetic energy into potential energy, which is permanently stored into elastic bands by means of a directional locking mechanism. The proposed approach has been validated through experiments, in comparison with a rigid manipulator. The results show that, compared with the case of a rigid manipulator, the proposed approach and the developed mechanical system achieve stable impact absorption without bouncing away from the interacting environment.**

I. Introduction

The number of civil applications in which unmanned aerial vehicles (UAVs) are used has grown rapidly over the past few years. Aerial robots are often solely used as an agile sensing platform, incapable of physically interacting with its environment. Contactless operations have already proved to be very valuable, however a large potential still lies in tasks that do require physical interaction.

Aerial vehicles that are able to physically interact with the environment, often called *Aerial Manipulators*, are a class of unmanned aerial vehicles that have the capability to perform physical interaction without the limitation of being constrained to the ground, meaning that they ideally possess an unbounded workspace.

Despite the strong expected impact of such technology within civil applications, technological challenges still need to be addressed. First of all, aerial manipulators are typically constituted by an underactuated floating base, implying that the system base is not directly actuated in all directions, causing that the aerial manipulator has to exploit its actuated degrees of freedom in order to generate motion along the non-actuated one. Moreover, the floating nature of the aerial manipulator adds control complexities in presence of moving masses and external disturbances introduced by the manipulation system itself. These issues have been recently studied in order to enable this technology to achieve tasks such as load transportation [1], collaborative physical interaction by means of multiple aerial manipulators carrying a shared load [2][3] and aerial grasping [4] [5] by means of robotic gripper that is directly mounted on the UAV base.

This work has been funded by the European Commission's H2020 project AEROWORKS under grant no. 644128 .

The authors are with the Faculty of Electrical Engineering, Mathematics and Computer Science, CTIT Institute, University of Twente, The Netherlands. Email: j.t.bartelds@student.utwente.nl,{s.hamaza, a.capra, s.stramigioli, m.fumagalli}@utwente.nl

Fig. 1: Aerial manipulator achieving stable interaction after an impact with a vertical surface.

However, when the aerial vehicle is equipped with a multi-degrees of freedom manipulator, additional challenges arise due to the coupled dynamics that originate between the aerial vehicle and the manipulator itself [6][7]. This phenomena sets strong limitations to the design of the manipulation system [8][9] and to the design of control methods that take into account the presence of a manipulator in the overall system dynamics [10] [11][12].

Another relevant issue related to the presence of a manipulator system on a UAV is the physical interaction at the end-effector of the robotic arm. In order to perform stable interaction while airborne, external forces have to be considered during the manipulation tasks [13][14]. Also in this case, the control of the aerial manipulator is a major issue [15], as a physical interaction with the environment can destabilize the system leading to undesired behaviours [7]. These studies have shown that stable control of the aerial manipulator, while physically interacting, can be achieved by means of proper control solutions. Nevertheless, one major limitation of these approaches is that the aerial manipulator performs aerial interaction in quasi-static situations. A solution to the problem of aerial interaction in which the UAV is not in near-hovering conditions has not been addressed yet.

This paper proposes an approach to the problem of dynamic physical interaction with the environment that is based on the analysis of the dynamic properties of mechanical systems interacting with the environment. The method presented

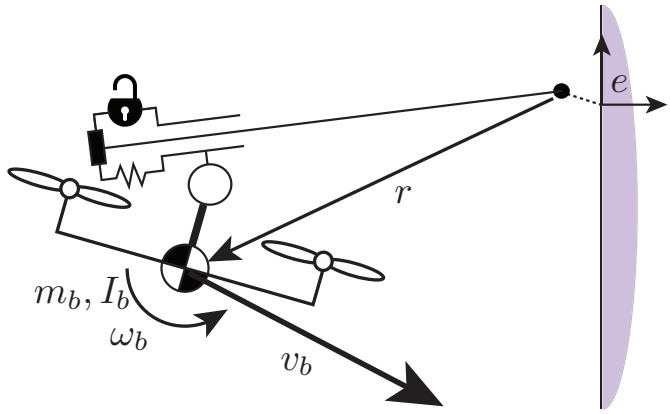

Fig. 2: Sketch of the proposed aerial manipulator design illustrating important properties. The concept consists of an actuated revolute joint and a linear passive degree of freedom with a locking mechanism.

in Section II focuses on the analysis of colliding systems towards the development of a new solution to the problem of handling impacts with an aerial manipulator. The proposed approach can be generalized to solve major issues in the field of aerial manipulation, and it has led to the development of a new design concept that is presented in Section III. An experimental validation of the theoretical approach is finally shown in Section IV, where the advantages compared to standard manipulator design concepts are highlighted and specifically tested in case of collision.

II. Method

Hereafter, we consider a multirotor UAV equipped with a generic manipulation system that allows sideways interaction with a vertical surface. Assuming that the manipulator mass and inertia are negligible compared to those of the UAV, the position of the total centre of mass of the aerial manipulator remains constant with respect to the UAV body fixed frame for any given relative motion of the manipulator with respect to the UAV.

We define m_b the total mass of the aerial manipulator and I_b the total inertia w.r.t the UAV centre of gravity (CoG).

In the proposed scenario the end-effector of the manipulator interacts with a vertical surface. The linear and angular momentum of the UAV, denoted as P and L respectively, relative to an inertial frame placed at the contact point can be expressed as:

$$\begin{bmatrix} P \\ L \end{bmatrix} = \begin{bmatrix} m_b v_b \\ I_b \omega_b + r \times m_b v_b \end{bmatrix} \tag{1}$$

being v_b and ω_b the linear and angular velocities of the aerial manipulator's CoG with respect to the inertia frame and r the distance vector of the manipulator's end-effector with respect to the centre of mass of the aerial manipulator.

If no external components act on the aerial manipulator's centre of mass, the momentum remains constant. Variation of the momentum are generally present due to gravitational terms, propellers' forces and moments, and external wrenches acting on the manipulator's end-effector. The variation of linear and angular momentum can therefore be formalized as follows:

$$\begin{bmatrix} \dot{P} \\ \dot{L} \end{bmatrix} = W_g + W_u + W_e \tag{2}$$

where W_g represents the wrench due to gravitational components, W_e is the external wrench generated by the interaction of the manipulator's end-effector with the environment, and W_u is the wrench generated by the propellers in the inertial frame, which is explicitly written as:

$$W_u = T_b W_u^b$$

being W_u^b the actuation wrench expressed in body-fixed frame, and $T_b \in \mathbb{R}^{6\times 6}$ a matrix that transforms the actuation wrench from body-fixed frame to inertial frame. Note that W_u^b can be modelled as a linear combination of the propellers' forces as:

$$W_u^b = \begin{bmatrix} 0 & 0 & 0 & 0 \\ 0 & 0 & 0 & 0 \\ 1 & 1 & 1 & 1 \\ 0 & -d & 0 & d \\ d & 0 & -d & 0 \\ -c & c & -c & c \end{bmatrix} \begin{bmatrix} f_1 \\ f_2 \\ f_3 \\ f_4 \end{bmatrix} \tag{3}$$

where c is an aerodynamic parameter of the propellers representing the inverse of the thrust to drag ratio and d is the distance from the propeller axis to the centre of the UAV. Note that (3) highlights the underactuation properties of a generic quadrotor UAV, showing that the UAV has not a direct control on the lateral components of the generated wrench in the body fixed frame. Therefore, the only way the UAV can react to the impulsive force generated impacting against the vertical surface is by tilting its attitude. Nevertheless, due to the impulsive nature of the impact both linear and angular momenta are subject to a drastic change, which makes the control of impacts using an underactuated floating base extremely challenging.

Our method proposes a way to minimize the effect of an impact on the UAV, such that the aerial manipulator remains in a controllable state both during and after the interaction. Moreover, we want to minimize bounces between the end-effector and the vertical surface caused by the reflection of linear momentum at impact. To do so, consider the aerial manipulator approaching a vertical wall with linear velocity $v_{b,i}$ and angular velocity $\omega_{b,i} \approx 0$. In the hypothesis of elastic impact, both linear and angular momentum as well as the total energy of the system are conserved.

Based on the above considerations, in order to achieve minimum variation of angular momentum, the contribution of the linear velocity to the angular momentum with respect to the interaction point has to be minimized during interaction. With an eye on Figure 2, and with reference to (1), this can be achieved by setting to zero the cross-product $r \times m_b v_b$, which implies that the distance vector from the

end-effector to the centre of mass of the aerial manipulator have to be aligned with the linear velocity vector.

Additionally, the energy balance of the system for the states before and after collision, denoted by subscripts i and f respectively, is examined.

Before impact, the total energy of the system only comprises the kinetic energy of the aerial manipulator. In the hypothesis that the angular velocity before impact is $\omega_{b,i} \approx 0$ and that $r \times m_b v_{b,i} \approx r \times m_b v_{b,f} \approx 0$, the energy balance reduces to:

$$\frac{1}{2} m_b v_{b,i}^2 = \frac{1}{2} m_b v_{b,f}^2 \tag{4}$$

Under these conditions, the momentum is reflected during the collision, i.e. $m_b v_{b,i} = -m_b v_{b,f}$. In order to prevent this reflection of the linear momentum, a mechanical storage element is used that decouples the position of the end-effector from the position of the aerial manipulator's centre of mass. The total energy of the system then becomes:

$$\frac{1}{2} m v_i^2 = \frac{1}{2} m v_f^2 + \frac{1}{2} k x^2 \tag{5}$$

being k the spring constant of the storage element and x the stroke induced by the impact force on the manipulator.

Note that the initial kinetic energy is transformed after impact into new kinetic energy and potential energy. In case the spring allows to store sufficient energy to compensate for the initial kinetic energy, then it results in $v_f = 0$. Nevertheless, a simple storage element does not fulfil the requirement of preventing the linear velocity to change direction. Therefore, in order to prevent the system from bouncing back, our approach is to use elastic storage elements in combination with a passive locking system that prevents the release of the stored energy. This can be achieved by choosing x as a monotonic function, which can be obtained by ensuring $\dot{x} \geq 0$ for any given wrench applied to the manipulator. Next sections show the mechanical choices that yield such properties and the experimental verification of the proposed approach.

III. Mechanical Design

A manipulation system has been developed to verify the proposed approach and test the capability of the aerial manipulator to achieve stable interaction after an impact. Hereafter the design of the manipulator is presented.

A. Manipulator Design

The manipulator system has been designed to be lightweight and compact, but also in a way that allows sideways interaction with the environment. To achieve this, the total payload and moving mass of the manipulator have been chosen such that they do not influence the flight stability of the UAV. The main body of the manipulator is placed close to the CoG, while a rod extends outside the rotors' area. An active rotational degree of freedom embodied by a servo motor decouples the pitch of the UAV from the pitch of the end-effector, i.e. to position the end-effector relative to the UAV CoG. The rod slides along its axis

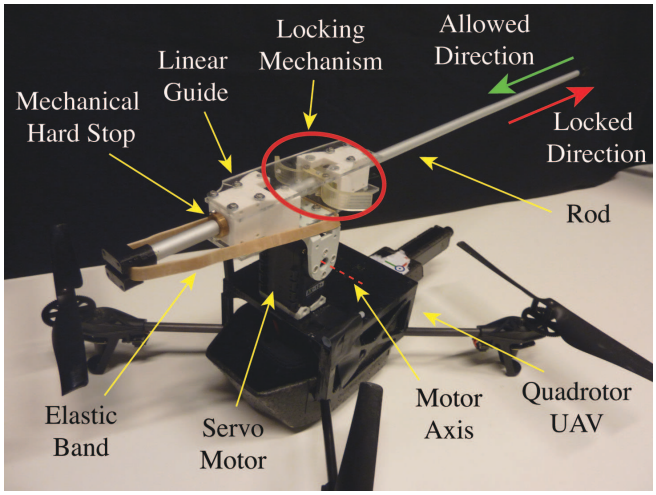

Fig. 3: Detail of the manipulator.

in a linear guide. A locking mechanism (see Section III-B for details) allows the motion of the latter into the linear guide in one direction, while it prevents the motion of the rod in the opposite direction. The rod is connected to its linear guide by means of an elastic band that acts as a spring. When an external force is applied on the end-effector along its axis and in the direction of the UAV, energy is stored into the elastic band. When no force is applied, or the force is in the opposite direction, a locking mechanism prevents the linear rod from sliding, and therefore it blocks the springs from releasing the stored potential energy. In case of impact with the environment, the kinetic energy of the collision is converted into potential energy, and permanently stored thanks to the locking mechanism. In order to release the potential energy, a manual lever has been designed on the locking mechanism, as shown in next section. Finally, a mechanical hard-stop is placed on the rod to provide a small pretensioning of the elastic bands at rest, such that the manipulation system does not have passive internal motion during free flight.

B. Locking Mechanism Design

The locking mechanism is a passive mechanical element that locks the motion of the rod in one direction, while allowing its motion in the opposite direction. With reference to Figures 4 and 5, the presence of teeth on each cam's profile allows for simultaneous rotation of the cams relatively to each other. The cam rotation is constrained on one side by the presence of the rod, while on the other side a spring connecting the two cams generates a torque that causes the cams to close on the rod. With reference to Figure 5, as the rod moves in one direction frictional components between the cams and the rod generate a torque that is opposite to the torque provided by the locking spring, allowing the motion of the rod. When the motion is in the opposite direction, the frictional components between the cams and the rod tend to close the cams, which consequently increase the friction

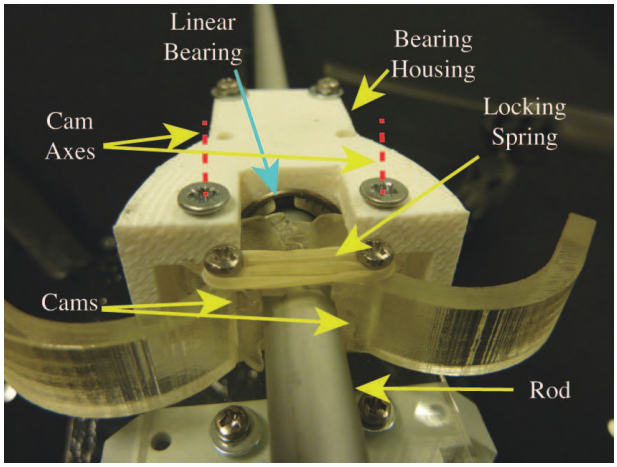

Fig. 4: Detail of the lock mechanism.

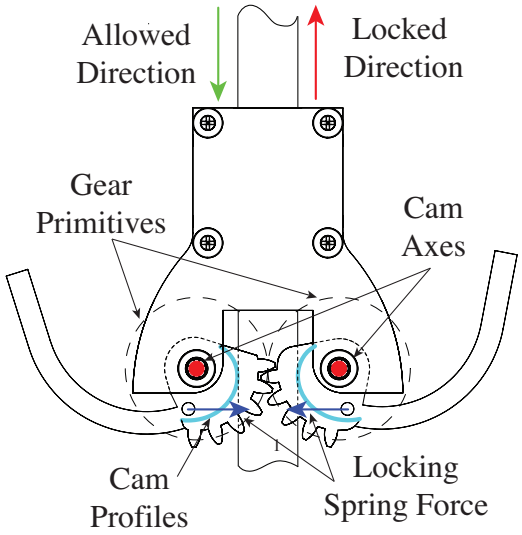

Fig. 5: Sketch of the cams system developed in the lock mechanism.

between the elements to the extent that motion of linear rod is blocked in that direction. [1]

IV. Experimental Validation

An experimental validation of the proposed approach is reported hereafter and compared to the case an impact occurs with a rigid manipulator. Firstly, the hardware components that have been used to perform the tests are described, then the realization of the control inputs to the system are shown, following the approach of Section II. Finally experimental results are presented.

A. Hardware Setup

Tests have been performed using the commercial platform ARDrone Parrot 2.0. This UAV has been selected for his availability, low price and easiness to be interfaced with ROS, in order to reduce time-to-test. The Parrot control system is considered as a black box whose functionality is to control the attitude of the UAV itself. Preliminary tests determined that the maximum payload the UAV can carry is about 300 grams when the protective case is mounted on the UAV and the weights are balanced around the CoG. Given these considerations, in order to maintain a good maneuverability, the maximum manipulator weight allowed has been set to 250 gram, and the protective case has been removed.

An ATI Mini 45 6 axis Force/Torque Sensor has been used to measure the forces exerted on a target wall. The Sensor is interfaced with the computer architecture via the ATI-NetFT box, which provides ethernet communication over the network. The sensor has been mounted on the vertical wall, between the wall itself and the target on which the UAV will achieve interaction. The target is constituted by a circle of 20 cm of radius, which allows measuring the interaction of the UAV and the target despite position uncertainties, while measured forces are within the sensor's calibrated area.

A Robotis dynamixel A-12A has been used as head mount for the manipulator, providing a rotational degree of freedom required to minimize variations in (1), as it will be shown in Section IV-B. This servo has been selected despite of its weight, which constitutes almost 30% of the allowed payload, because it does not require additional electronics or control and is straightforward to interface with ROS via serial communication.

The manipulator's end-effector, i.e. the rod presented in Section III, is an aluminum tube of 1 m length that allows the UAV to interact with the environment sideways, providing a maximum stroke of 30 cm before the propellers touch the vertical environment at 0° of pitch. The overall weight of the manipulator, including the servo motor and the components necessary for mounting the manipulator on the UAV, is around 240 grams.

A motion capture system, the NaturalPoint Optitrack system, is used to measure relevant position and orientation data during the experiments.

B. Test Implementation

The experiments that have been performed are meant to compare the behaviour of a rigid manipulator with our manipulator prototype. In both cases, the UAV is controlled to move towards a vertical wall at constant pitch. As described in Section II, in order to reduce momentum variation at the time of interaction, the cross product in (1) is minimized using the dynamixel servo to keep the end effector tip in a position such that:

$$\frac{p_e - p_{CoG}}{\|p_e - p_{CoG}\|} = \frac{v_{CoG}}{\|v_{CoG}\|} \tag{6}$$

being p_e and p_{CoG} the position in the inertial frame of the end effector and the centre of gravity of the aerial manipulator, and v_{CoG} its linear velocity. Note that the position of the CoG is considered fixed, even if during the impact it changes slightly due to the moving rod, and has been estimated by hanging the drone on a wire.

Throughout the experiments the dynamixel's dynamics have been considered as an unitary gain and we assumed that its embedded controller provides angle control with infinite

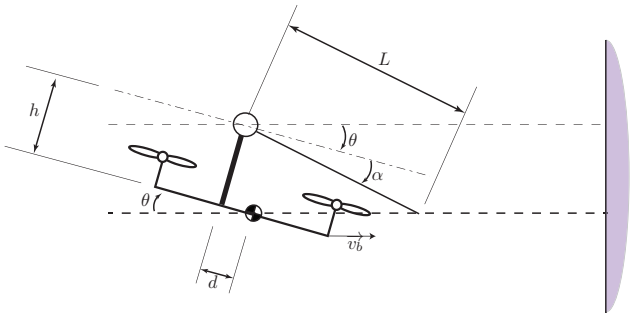

Fig. 6: Centre of Gravity lever arm minimization frame of reference

resolution. With reference to Figure 6 the commanded angle α that is assigned as a position reference to the dynamixel servo motor is computed as:

$$\alpha = \arcsin\left(\frac{d\,\sin\theta + h\,\cos\theta}{L}\right) - \theta \qquad (7)$$

where θ is the real-time pitch derived from the motion capture module. To simplify test execution the drone's velocity vector has been kept perpendicular to the wall plane.

In order to ensure repeatable tests and acquire valuable data, the test has been scripted such that the drone is autonomously following the sequence:

1) Take off
2) Hover at initial position
3) Enable servo to minimize lever-arm
4) Approach target with constant pitch
5) Maintain contact with target for about 1 second
6) Return to hover position and land

This sequence allowed to repeat and compare the test performed with the rigid manipulator and the one that utilized the mechanism developed within this work.

C. Experimental Results

This section shows some experimental results for two type of manipulator set-ups: one manipulator consists of the compliant rod with locking mechanism (CL) as reported in Section III, the second consists of a rod that is rigidly connected to the output of the servo motor mounted on the aerial vehicle, which therefore behaves as an ideal infinitely-stiff linear degree of freedom, meaning that it cannot store kinetic energy into potential. In all of the timeseries presented, the time coordinates have been zeroed with respect the impact time.

Figure 7 shows that the interaction with the vertical wall causes loss of contact between the end-effector and the wall, resulting in the aerial vehicle bouncing half a meter away from the target. When the CL setup is used it is possible to maintain a stable contact with the wall, meaning that the attitude controller is not lead to a condition that provokes loss of controllability. Note that Figure 7 reveals a significant

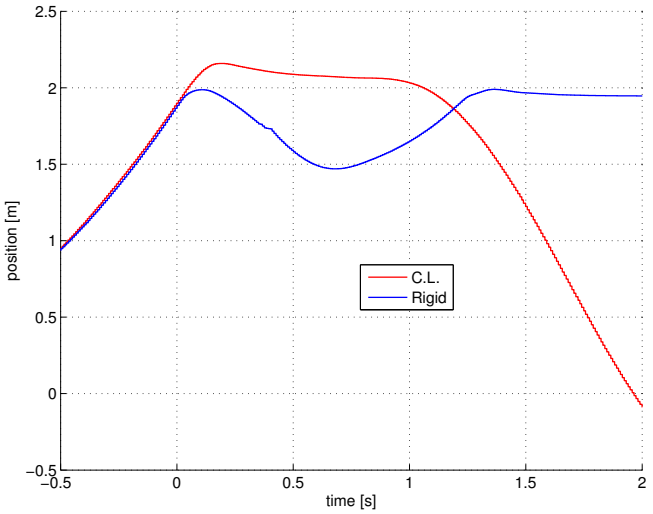

Fig. 7: UAV position along the approach direction. When the rigid manipulator has been used the aerial manipulator crashed after 1.5 s due to the induced instabilities; when the compliant manipulator has been used the aerial manipulator is able to maintain contact and then land safely

difference in the maximum reached UAV position: this is due to the manipulator compliance that allows the UAV to get closer to the vertical wall compared to the case in which the rigid manipulator is engaged. Note that the wall is positioned 2.40 meters from the origin of the reference frame of the tracking system. One second after the interaction occurs it can be noted that the UAV using the proposed mechanism is able to reposition itself at the starting position, while the rigid aerial manipulator crashes around 1.5s because of the destabilization induced by the high impact force.
Within the same experiment, Figure 8 shows the effect of the impact on the aerial manipulator's pitch using the two configurations. When the CL setup is engaged, the effect is negligible, and small deviations can be accounted for the imperfect CoG compensation. On the other hand, when using the rigid setup, a quick UAV's pitch change due to the high interaction force causes the attitude controller destabilization, to the extent that the aerial vehicle is not able neither to maintain a stable contact with the target, nor to recover quickly from the shock due to the impact. This is mainly due to the fact that the dynamixel servo is not infinitely rigid and cannot counteract the force exerted at the time of impact, yielding to the drone's pitch increase. As such, the presented compliant setup is capable of minimizing both the bouncing effect and the tilting force.

Figure 9 shows the exerted forces on the target along the approach direction, that is the direction perpendicular to the wall plane. It is clear that when interacting using the rigid manipulator all the momentum gained by the aerial manipulator is transferred to the wall, resulting in a high impulsive force. When using the CL manipulator the energy transferred to the wall is sensibly decreased due to the energy stored into the spring (see table I).

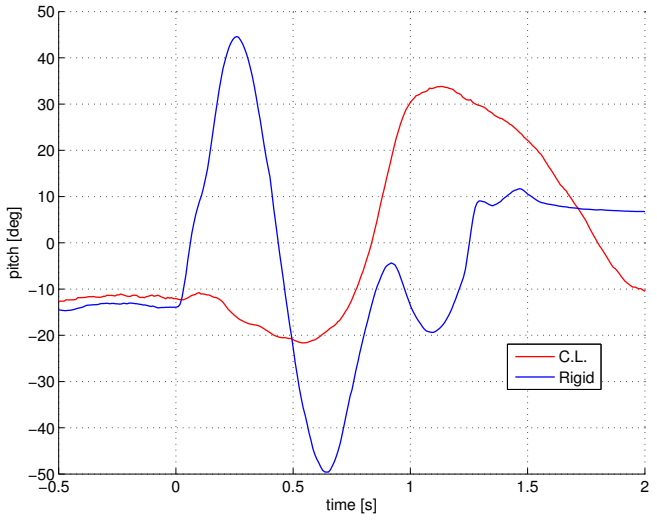

Fig. 8: Aerial manipulator's measured pitch. In this figure a negative pitch reflects the UAV flying towards the target. The pitch increase for the CL data is due to the aerial manipulator detaching from the wall.

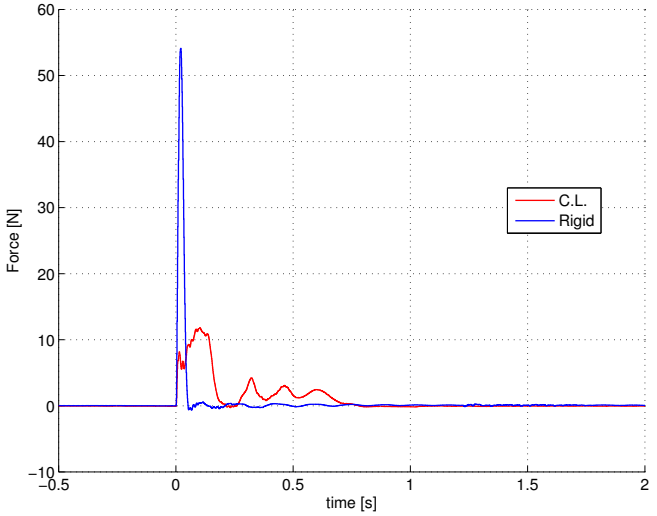

Fig. 9: Forces exerted on the target. When a rigid manipulator is used a high force is exerted due to the sudden momentum variation. Using the proposed compliant manipulator results in a lower force. The oscillations shown are due to the UAV black-boxed attitude control, which is not tuned to interact with the environment.

This result opens the way for compliant aerial manipulators as a means to dynamic aerial interaction with the environment.

V. Conclusion

The paper proposed the design of a manipulator capable of handling aerial impacts, without requiring any modifications to the flight controller of the UAV. The success of the design relies on two majour concepts. Firstly, the contact location is positioned by means of an active degree of freedom, such that the generated angular momentum is minimized and consequentially the UAVs attitude remains controllable. Secondly, a system that irreversibly extracts the kinetic energy at impact is conceptualized in order to prevent linear momentum from being reflected. The experiment demonstrates the first achievement in the regime of highly dynamic aerial interactions, which paves the way to the next generation of Aerial Robotic Workers.

Mode	$\|F\|_\infty$
Compliant + Lock	$11.8N$
Rigid	$54.2N$

TABLE I: Peak forces

References

[1] I. Palunko, P. Cruz, and R. Fierro, "Agile load transportation : Safe and efficient load manipulation with aerial robots," *Robotics Automation Magazine, IEEE*, vol. 19, no. 3, pp. 69–79, Sept 2012.

[2] M. Bernard and K. Kondak, "Generic slung load transportation system using small size helicopters," in *2009 IEEE International Conference on Robotics and Automation, ICRA 2009, Kobe, Japan, May 12-17, 2009*, 2009, pp. 3258–3264. [Online]. Available: http://dx.doi.org/10.1109/ROBOT.2009.5152382

[3] N. Michael, J. Fink, and V. Kumar, "Cooperative manipulation and transportation with aerial robots," *Autonomous Robots*, vol. 30, no. 1, pp. 73–86, 2011. [Online]. Available: http://dx.doi.org/10.1007/s10514-010-9205-0

[4] P. E. Pounds, D. Bersak, and A. Dollar, "Grasping from the air: Hovering capture and load stability," in *Robotics and Automation (ICRA), 2011 IEEE International Conference on*, May 2011, pp. 2491–2498.

[5] D. Mellinger, Q. Lindsey, M. Shomin, and V. Kumar, "Design, modeling, estimation and control for aerial grasping and manipulation," in *Intelligent Robots and Systems (IROS), 2011 IEEE/RSJ International Conference on*, Sept 2011, pp. 2668–2673.

[6] F. Huber, K. Kondak, K. Krieger, D. Sommer, M. Schwarzbach, M. Laiacker, I. Kossyk, S. Parusel, S. Haddadin, and A. Albu-Schaffer, "First analysis and experiments in aerial manipulation using fully actuated redundant robot arm," in *Intelligent Robots and Systems (IROS), 2013 IEEE/RSJ International Conference on*, Nov 2013, pp. 3452–3457.

[7] K. Kondak, K. Krieger, A. Albu-Schaeffer, M. Schwarzbach, M. Laiacker, I. Maza, A. Rodriguez-Castano, and A. Ollero, "Closed-loop behavior of an autonomous helicopter equipped with a robotic arm for aerial manipulation tasks," *International Journal of Advanced Robotic Systems*, vol. 10, no. 145, pp. 1–9, February 2013. [Online]. Available: http://dx.doi.org/10.5772/53754

[8] A. Keemink, M. Fumagalli, S. Stramigioli, and R. Carloni, "Mechanical design of a manipulation system for unmanned aerial vehicles," in *Robotics and Automation (ICRA), 2012 IEEE International Conference on*, May 2012, pp. 3147–3152.

[9] K. Kondak, F. Huber, M. Schwarzbach, M. Laiacker, D. Sommer, M. Bejar, and A. Ollero, "Aerial manipulation robot composed of an autonomous helicopter and a 7 degrees of freedom industrial manipulator," in *Robotics and Automation (ICRA), 2014 IEEE International Conference on*, May 2014, pp. 2107–2112.

[10] A. Jimenez-Cano, J. Martin, G. Heredia, A. Ollero, and R. Cano, "Control of an aerial robot with multi-link arm for assembly tasks," in *Robotics and Automation (ICRA), 2013 IEEE International Conference on*, May 2013, pp. 4916–4921.

[11] C. Korpela, M. Orsag, T. Danko, B. Kobe, C. McNeil, R. Pisch, and P. Oh, "Flight stability in aerial redundant manipulators," in *Robotics and Automation (ICRA), 2012 IEEE International Conference on*, May 2012, pp. 3529–3530.

[12] C. Korpela, M. Orsag, M. Pekala, and P. Oh, "Dynamic stability of a mobile manipulating unmanned aerial vehicle," in *Robotics and Automation (ICRA), 2013 IEEE International Conference on*, May 2013, pp. 4922–4927.

[13] M. Fumagalli, R. Naldi, A. Macchelli, R. Carloni, S. Stramigioli, and L. Marconi, "Modeling and control of a flying robot for contact inspection," in *Intelligent Robots and Systems (IROS), 2012 IEEE/RSJ International Conference on*, Oct 2012, pp. 3532–3537.

[14] J. Scholten, M. Fumagalli, S. Stramigioli, and R. Carloni, "Interaction control of an uav endowed with a manipulator," in *Robotics and Automation (ICRA), 2013 IEEE International Conference on*, May 2013, pp. 4910–4915.

[15] M. Fumagalli, R. Naldi, A. Macchelli, F. Forte, A. Keemink, S. Stramigioli, R. Carloni, and L. Marconi, "Developing an aerial manipulator prototype: Physical interaction with the environment," *Robotics Automation Magazine, IEEE*, vol. 21, no. 3, pp. 41–50, Sept 2014.